

Stochastic models of polymeric fluids at small Deborah number

T. Li ^{1,*}, E. Vanden-Eijnden ^{2,4}, P. Zhang ¹, and W. E ^{3,4}

¹*LMAM and School of Mathematical Sciences, Peking University, Beijing 100871, P.R.China*

²*Courant Institute, New York University, New York, NY 10012, USA*

³*Department of Mathematics and PACM, Princeton University, Princeton, NJ 08544, USA*

⁴*School of Mathematics, Institute for Advanced Study, Princeton, NJ 08540, USA*

Abstract

Stochastic models are considered as a numerical tool for simulating the dynamic behavior of polymeric fluids. At small Deborah number, straightforward numerical integration of these models is both costly because of the separation of time scales and inaccurate because of the large numerical fluctuation. A new technique, motivated by the recently developed heterogeneous multi-scale method (HMM), is introduced to overcome these problems.

Keywords: Brownian configuration fields (BCF); Dumbbell model; Heterogeneous multi-scale method (HMM); Stochastic multi-scale decomposition

1 Introduction

Stochastic models of polymeric fluids have attracted a great deal of attention in recent years [9]. Compared with traditional hydrodynamic models which rely on sophisticated constitutive relations to represent the polymeric nature of the fluid, stochastic models have the advantage of bypassing empirical constitutive relations and at the same time provide a direct link between the conformation of the polymers and the behavior of the fluid.

In this paper, we will focus on the Brownian Configuration Fields (BCF) model of polymeric fluids introduced by Hulsen et al. [7]. The simplest example of such

*Corresponding author. Email: tieli@pku.edu.cn

a model is the dumbbell model in which the polymers are modelled as dumbbells each of which consists of two beads connected by a spring. The configuration of the dumbbell is specified by the positional vectors of the spring, denoted by \mathbf{Q} . In the BCF model \mathbf{Q} is a random vector field, the ensemble of which represents the ensemble of configurations of the dumbbells. The dumbbells are convected and stretched by the flow and at the same time experiences the spring and Brownian forces:

$$\frac{\partial \mathbf{Q}}{\partial t} + (\mathbf{u} \cdot \nabla) \mathbf{Q} = \kappa \mathbf{Q} - \frac{1}{2De} \mathbf{F}(\mathbf{Q}) + \frac{1}{\sqrt{De}} \dot{\mathbf{W}}(t). \quad (1)$$

Here $\kappa = (\nabla \mathbf{u})^T$, $\mathbf{F}(\mathbf{Q})$ is the spring force, De is the Deborah number, which measures the relative importance between elastic and convective effects, and $\dot{\mathbf{W}}(t)$ is a temporal white-noise modeling thermal effects; \mathbf{u} is the velocity field, which satisfies the momentum equation and incompressibility condition:

$$\frac{\partial \mathbf{u}}{\partial t} + (\mathbf{u} \cdot \nabla) \mathbf{u} + \nabla p = \frac{\gamma}{Re} \Delta \mathbf{u} + \frac{1-\gamma}{ReDe} \nabla \cdot \tau_p, \quad \nabla \cdot \mathbf{u} = 0, \quad (2)$$

where Re is the Reynolds number, γ is the ratio between solvent and polymer viscosities and τ_p is the extra stress due to the polymers. In the dilute limit, this polymeric stress is given by Kramers expression:

$$\tau_p = -I + \bar{\tau}_p, \quad \bar{\tau}_p = \langle \mathbf{F}(\mathbf{Q}) \otimes \mathbf{Q} \rangle \quad (3)$$

where \otimes denotes tensor product, and $\langle \cdot \rangle$ denotes averaging with respect to thermal noise; noting that $\nabla \cdot \tau_p = \nabla \cdot \bar{\tau}_p$, we only need to evaluate $\bar{\tau}_p$ in the fluid equation. For clarity we have expressed (1), (2) and (3) in appropriate non-dimensional units.

In practice, the stochastic field $\mathbf{Q}(\mathbf{x}, t)$ is represented by N replicas, $\{\mathbf{Q}_i(\mathbf{x}, t)\}_{i=1}^N$, each of which evolves according to (1) with an independent white-noise; the extra stress in (3) is then computed through ensemble averaging over the N configuration fields at each grid point as

$$\bar{\tau}_p \approx \frac{1}{N} \sum_{i=1}^N \mathbf{F}(\mathbf{Q}_i) \otimes \mathbf{Q}_i. \quad (4)$$

Compared with previous methods such as the CONNFFESSIT (Calculation Of Non-Newtonian Flow: Finite Elements and Stochastic Simulation Technique) [8], in which the polymers are represented by individual dumbbells, this approach eliminates the problem with the non-uniform distribution of the dumbbells, and at the same time reduces the variance in the computed velocity field.

In spite of this, BCF remains computationally too expensive in interesting situations when the Deborah number is small, for two reasons. First, there is a time-scale issue; while we are mainly interested in the behavior of the flow at the convective time scale, say, T_c , in simulations we are forced to deal with the much smaller elastic time scale, say, T_r , because of the model we use. Since $T_r = O(De)$ as $De \rightarrow 0$ from (1), whereas $T_c = O(1)$ from (2) (using $\tau_p = O(De)$, see (6) below), the number of time-steps necessary to reach the convective time-scale diverges as De^{-1} . Second, there is an accuracy issue in computing the average in (3) which defines the stress τ_p because $-I + \mathbf{F}(\mathbf{Q}) \otimes \mathbf{Q}$ has a small mean of order De but a large variance of order 1 and therefore the numerical solutions based directly on (1) suffer from large fluctuations when De is small. The order of magnitude of τ_p for small De can be estimated as follows. Using the Giesekus expression for τ_p , we have for $\mathbf{C}_Q := \langle \mathbf{Q} \otimes \mathbf{Q} \rangle$:

$$\frac{\partial \mathbf{C}_Q}{\partial t} + (\mathbf{u} \cdot \nabla) \mathbf{C}_Q = \kappa \mathbf{C}_Q + \mathbf{C}_Q \kappa^T - \frac{1}{De} \tau_p, \quad (5)$$

from which it can be deduced that

$$\tau_p = O(De), \quad (6)$$

as $De \rightarrow 0$. Since the error squared in the computation of $\tau_p = -I + \bar{\tau}_p$ via (4) can be estimated as

$$\text{error}^2 = \frac{\text{var}\{\mathbf{F}(\mathbf{Q}) \otimes \mathbf{Q}\}}{N}, \quad (7)$$

where, from (1), $\text{var}\{\mathbf{F}(\mathbf{Q}) \otimes \mathbf{Q}\}$ is typically $O(1)$ in De , it follows that the number N of realizations necessary to obtain an accurate estimate of τ_p via (4) diverges as De^{-2} for small De .

These problems have been noted in the review article of Suen et al. [14]. From a physical point of view, at small De , the relaxation time for the springs is much shorter than the convective time scale. Hence the fluid stays near equilibrium. In principle, this property can be used to obtain closures for the model by deriving effective constitutive relation. Indeed this can be easily done for BCF. In practice, however, such a procedure may become too complicated if more realistic polymer models are used. Therefore we will concentrate on analytical and numerical procedures that can be readily extended to more complicated polymer models.

In this paper we combine two techniques to overcome the numerical difficulties with the stochastic models at small Deborah number. The first is a variance reduction technique that extracts the dominant fluctuating terms from the polymeric

stress through a decomposition of \mathbf{Q} . In this formulation, two auxiliary fields are used to represent \mathbf{Q} , and (1) is enlarged into two equations for these fields. Similarly, the empirical average in (4) can be re-expressed in terms of the auxiliary fields. This eliminates the accuracy problem of (4). Variance reduction techniques of this type were already used in [10, 2] and, in a more general context, in [15]. This formulation also allows us to compute the zero Deborah number limit of (1), (2), and show that the field is Newtonian in this limit, but with a renormalized viscosity. The second technique is a multi-scale numerical method that deals with the problem of time-scale separation. The essence is to compute the evolution of \mathbf{Q} and \mathbf{u} using different time-steps (and different discretization in time) on different time intervals which are adapted to the natural time-scales on which these fields evolve. In particular, the evolution of the auxiliary fields \mathbf{Q} needs only to be computed on time-intervals of the order of T_r , yet the technique allows us to access the evolution of \mathbf{u} on time intervals of the order T_c .

While the techniques we introduce are general, in the numerical tests we will focus on two special cases of the spring force in (1); the Hookean model for which

$$\mathbf{F}(\mathbf{Q}) = \mathbf{Q}, \quad (8)$$

and the FENE model for which

$$\mathbf{F}(\mathbf{Q}) = \frac{\mathbf{Q}}{1 - Q^2/Q_0^2}, \quad (Q^2 < Q_0^2) \quad (9)$$

where $Q^2 = |\mathbf{Q}|^2$. Notice that both forces are potential, $\mathbf{F}(\mathbf{Q}) = \nabla_{\mathbf{Q}}V(Q)$, with $V(Q) = \frac{1}{2}Q^2$ and $V(Q) = -\frac{1}{2}Q_0^2 \log(1 - Q^2/Q_0^2)$, respectively. Notice also that, for Hookean dumbbells, we can derive a closed equation for the polymer stress:

$$\tau_p + De \overset{\nabla}{\bar{\tau}}_p = 0 \quad (10)$$

where $\bar{\tau}_p = \tau_p + \mathbf{l}$, and $\overset{\nabla}{\bar{\tau}}_p$ is the Oldroyd derivative of $\bar{\tau}_p$, which is defined as:

$$\overset{\nabla}{\bar{\tau}}_p = \frac{\partial \bar{\tau}_p}{\partial t} + (\mathbf{u} \cdot \nabla) \bar{\tau}_p - \kappa \cdot \bar{\tau}_p - \bar{\tau}_p \cdot \kappa^T.$$

In terms of $\bar{\tau}_p$, (10) is

$$\nabla \cdot \bar{\tau}_p = \nabla \cdot \tau_p, \quad \bar{\tau}_p + De \overset{\nabla}{\bar{\tau}}_p = \mathbf{l}, \quad (11)$$

which is the well-known Oldroyd-B model for polymeric fluids [1].

2 A new numerical implementation of BCF

Here we introduce an efficient numerical scheme for BCF in the small Deborah number regime. This is done in two steps; first, BCF is appropriately reformulated to eliminate the accuracy problem with the expression in (3) for the stress. This is done via the introduction of auxiliary fields to represent \mathbf{Q} following the ideas for variance reduction proposed in [2, 10] (see also [15]). Second, we introduce a numerical scheme for the new formulation of BCF to deal with the issue of time scale separation. The overall scheme uses the techniques introduced in [4, 15] to deal with dynamical systems with multiple time-scale and fits well the systematic framework of the heterogeneous multi-scale methods (HMM) proposed in [5].

2.1 Variance reduction using auxiliary fields

We write $\mathbf{Q}(\mathbf{x}, t)$ in the form

$$\mathbf{Q}(\mathbf{x}, t) = \bar{\mathbf{Q}}(t) + De \mathbf{q}(\mathbf{x}, t), \quad (12)$$

where $\bar{\mathbf{Q}}(t)$ is the solution of

$$\frac{d\bar{\mathbf{Q}}}{dt} = -\frac{1}{2De} \mathbf{F}(\bar{\mathbf{Q}}) + \frac{1}{\sqrt{De}} \dot{\mathbf{W}}(t). \quad (13)$$

From (1), (12), and (13), it is then easy to see using $\nabla \bar{\mathbf{Q}} = 0$ that $\mathbf{q}(\mathbf{x}, t)$ satisfies

$$\frac{\partial \mathbf{q}}{\partial t} + (\mathbf{u} \cdot \nabla) \mathbf{q} = \frac{1}{De} \kappa(\bar{\mathbf{Q}} + De \mathbf{q}) - \frac{1}{2De} \mathbf{G}(\bar{\mathbf{Q}}, \mathbf{q}, De), \quad (14)$$

where

$$\mathbf{G}(\bar{\mathbf{Q}}, \mathbf{q}, De) = \int_0^1 (\mathbf{q} \cdot \nabla_{\bar{\mathbf{Q}}}) \mathbf{F}(\bar{\mathbf{Q}} + De\theta \mathbf{q}) d\theta. \quad (15)$$

(13) and (14) are strictly equivalent to (1) via (12).

On the other hand, we also have

$$\frac{1}{De} \tau_p = \langle \mathbf{F}(\bar{\mathbf{Q}}) \otimes \mathbf{q} \rangle + \langle \mathbf{G}(\bar{\mathbf{Q}}, \mathbf{q}, De) \otimes \bar{\mathbf{Q}} \rangle + De \langle \mathbf{G}(\bar{\mathbf{Q}}, \mathbf{q}, De) \otimes \mathbf{q} \rangle, \quad (16)$$

where we used that $\langle \mathbf{F}(\bar{\mathbf{Q}}) \otimes \bar{\mathbf{Q}} \rangle$ depends only on t from (13). The rescaled stress, τ_p/De , which enters (2) can now be computed directly from (16). The terms at the right hand side of (16) are $O(1)$ in De and therefore do not suffer from the same

accuracy problem as (4). With N replica fields of $\bar{\mathbf{Q}}, \mathbf{q}, \{\bar{\mathbf{Q}}_i, \mathbf{q}_i\}_{i=1}^N$, this amounts to estimating (16) using

$$\frac{1}{De} \tau_p \approx \frac{1}{N} \sum_{i=1}^N (\mathbf{F}(\bar{\mathbf{Q}}_i) \otimes \mathbf{q}_i + \mathbf{G}(\bar{\mathbf{Q}}_i, \mathbf{q}_i, De) \otimes \bar{\mathbf{Q}}_i + De \mathbf{G}(\bar{\mathbf{Q}}_i, \mathbf{q}_i, De) \otimes \mathbf{q}_i). \quad (17)$$

From now on, we shall compute with the new system (2), (13), (14), and (16); in the appendix, we also show that this system can be used to deduce the zero Deborah limit of BCF.

2.2 Dealing with the separation of time scales

We now consider the problem due the disparity between the microscopic relaxation time scale $T_r = O(De)$, and the macroscopic convective time scale $T_c = O(1)$ (in De ; in fact, $T_c = O(Re)$ in De, Re). We will refer to T_r as the micro-time-scale and T_c as the macro-time-scale. Since we are mainly interested in the macro-time-scale, we will solve the hydrodynamic equation in (2) for \mathbf{u} using a macro time step Δt_c . However to obtain τ_p , we need to solve the equations in (13) and (14) for $\bar{\mathbf{Q}}$ and \mathbf{q} using a much smaller micro-time-step Δt_r . The key observation is that because the relaxation time of $\bar{\mathbf{Q}}$ and \mathbf{q} is short compared with Δt_c , (13) and (14) only need to be solved on a time interval which is much smaller than the macro-time-step in order to provide accurate enough estimates for τ_p . The overall time stepping strategy then uses a grid illustrated in Fig. 1.

To summarize, the overall numerical procedure consists of two components:

1. Solve the equation for \mathbf{u} in (2) on the macro-time-step using standard ODE solvers, such as Runge-Kutta.
2. At each macro-time-step or Runge-Kutta stage, estimate τ_p from (16) by solving the equations for $\bar{\mathbf{Q}}$ and \mathbf{q} in (13) and (14) with \mathbf{u} fixed using micro-time-steps until the empirically computed τ_p reaches a quasi-stationary value.

To obtain better statistics, we use time averages (after the configuration fields \mathbf{Q} become statistically stationary) in addition to ensemble averaging. Since this scheme fits within the HMM framework, we shall simply refer to it as such.

A further simplification can be obtained if we note the fact that, because $\bar{\mathbf{Q}}$ does not depend on \mathbf{u} , it can in principle be computed only once. In particular, this means that one could (i) obtain once and for all a representative ensemble of

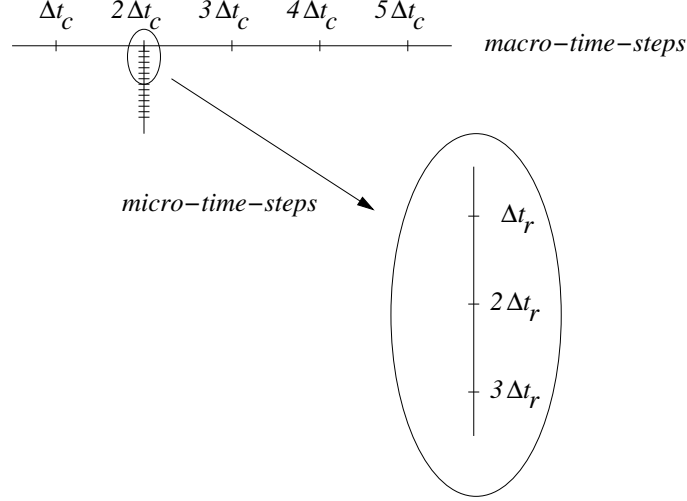


Figure 1: Sketch of time stepping procedure.

time-independent random variable \bar{Q}_i on the invariant measure of the process $\bar{\mathbf{Q}}(t)$, then (ii) estimate τ_p via algebraic solution of (14) – i.e. obtain the steady solution of this equation, $\partial \mathbf{q} / \partial t = 0$ – at given \mathbf{u} and for each fixed \bar{Q}_i .

3 Numerical tests on shear flows

It is instructive to look at the special case of pressure driven shear flows in two dimension, for which

$$\mathbf{u}(x, y) = \begin{pmatrix} u(y) \\ 0 \end{pmatrix}, \quad \nabla p = \begin{pmatrix} c \\ 0 \end{pmatrix}, \quad (18)$$

with c prescribed. In this case, it is easy to check that the original equations in (1), (2) reduce to

$$\begin{cases} \frac{\partial Q_1}{\partial t} = \frac{\partial u}{\partial y} Q_2 - \frac{1}{2De} F_1(\mathbf{Q}) + \frac{1}{\sqrt{De}} \dot{W}_1 \\ \frac{\partial Q_2}{\partial t} = -\frac{1}{2De} F_2(\mathbf{Q}) + \frac{1}{\sqrt{De}} \dot{W}_2 \\ \frac{\partial u}{\partial t} + c = \frac{\gamma}{Re} \frac{\partial^2 u}{\partial y^2} + \frac{1-\gamma}{ReDe} \frac{\partial}{\partial y} \langle F_2(\mathbf{Q}) Q_1 \rangle. \end{cases} \quad (19)$$

These equations can be reformulated in terms of the auxiliary fields (12); though we consider both the Hookean and the FENE models in the numerical tests below, we only give these equations explicitly for the Hookean model, where they take a

particularly simple form due to the linearity of the forcing which implies $Q_2 = \bar{Q}_2$, $q_2 = 0$:

$$\begin{cases} \frac{\partial \bar{Q}_1}{\partial t} = -\frac{1}{2De} \bar{Q}_1 + \frac{1}{\sqrt{De}} \dot{W}_1 \\ \frac{\partial q_1}{\partial t} = \frac{1}{De} \frac{\partial u}{\partial y} Q_2 - \frac{1}{2De} q_1 \\ \frac{\partial Q_2}{\partial t} = -\frac{1}{2De} Q_2 + \frac{1}{\sqrt{De}} \dot{W}_2 \\ \frac{\partial u}{\partial t} + c = \frac{\gamma}{Re} \frac{\partial^2 u}{\partial y^2} + \frac{1-\gamma}{Re} \frac{\partial}{\partial y} \langle q_1 Q_2 \rangle. \end{cases} \quad (\text{Hookean}) \quad (20)$$

In Figures 2-6 we present some numerical results on this model. The domain of the channel is taken to be $y \in [0, 1]$. The parameters are chosen as $Re = 1$, $c = -1$, $\gamma = \frac{1}{9}$, and we used 250 configuration fields. The initial data are set as $u|_{t=0} = 0$, $Q_i|_{t=0} = N(0, 1)$ which are independent standard normal random variables. The initial data for augmented system are

$$\bar{Q}_{1,i}|_{t=0} = N(0, 1), \quad Q_{2,i}|_{t=0} = N(0, 1), \quad q_{1,i}|_{t=0} = 0.$$

Both the Hookean and FENE models are computed to test the effectiveness of the approach. MAC scheme is used to discretize the momentum equation [12], and the Euler scheme is used to discretize the SDEs [13]. For FENE, the rejection method is used [9]. The maximal extension of the spring is set at $Q_0^2 = 100$. We reject all moves which lead to a value of Q^2 that exceeds 75 percent of the maximal extension Q_0^2 . Numerical experience suggests that rejection occurs very rarely.

In order to better calibrate the statistical error in BCF, we also compute the solution for the Hookean model with that of the Oldroyd-B model. The two should be the same in the absence of statistical error.

Numerical Test 1: Original system (19). Shown in Figure 2 is the numerical result using directly the original BCF model. We see a large error in the transient regime.

Numerical Test 2: Augmented system (20). In Figures 3 and 4 we present the numerical results for the Hookean model at $De = 10^{-3}$ using the auxiliary fields. We see that the large error in the transient regime is eliminated. HMM is not used in these results.

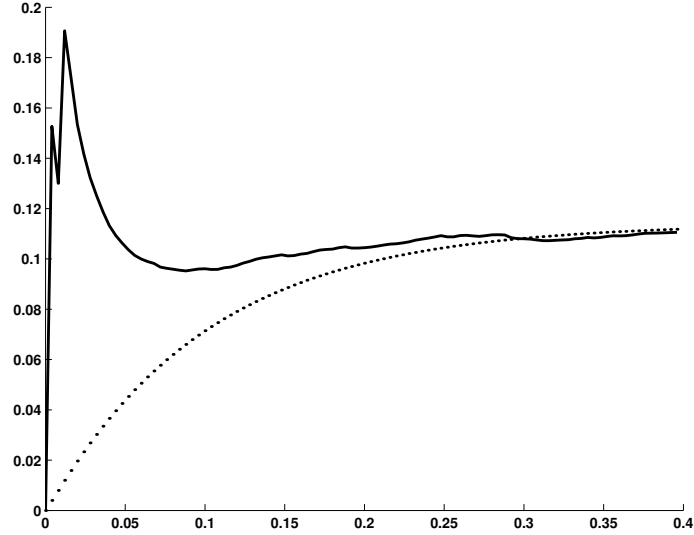


Figure 2: Time history of u at the middle point of the channel $y = \frac{1}{2}$. Solid line is the result of Hookean model, dotted line is the result from Oldroyd-B equation. $De = 10^{-3}$, $Re = 1$, $\gamma = \frac{1}{9}$. Note the large error in the transient regime.

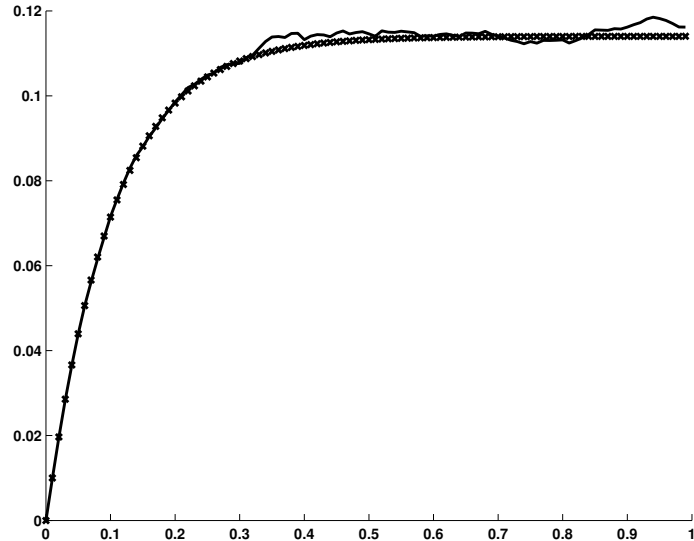


Figure 3: Time history of u at the middle point of the channel $y = \frac{1}{2}$. Solid line is the result of Hookean model, dotted line is the result from Oldroyd-B equation. $De = 10^{-3}$, $Re = 1$, $\gamma = \frac{1}{9}$. The large error in the transient regime is now eliminated.

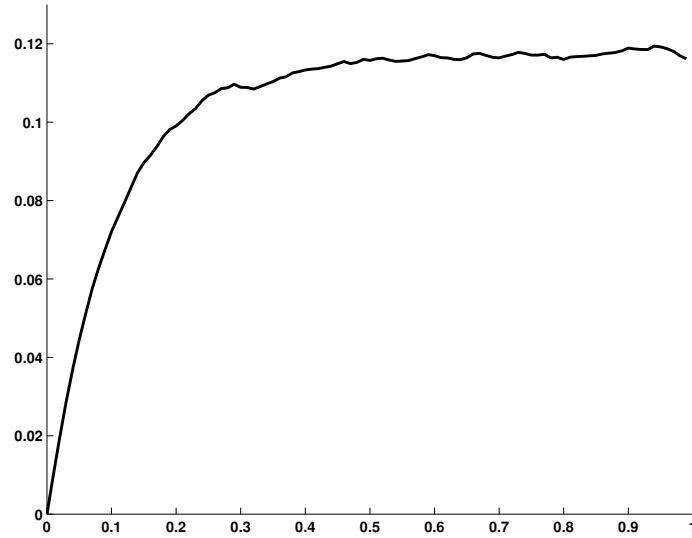


Figure 4: Time history of u at the middle point of the channel $y = \frac{1}{2}$ for the FENE model. $Q_0^2 = 100$, $De = 10^{-3}$, $Re = 1$, $\gamma = \frac{1}{9}$. Again there is no large error in the transient regime.

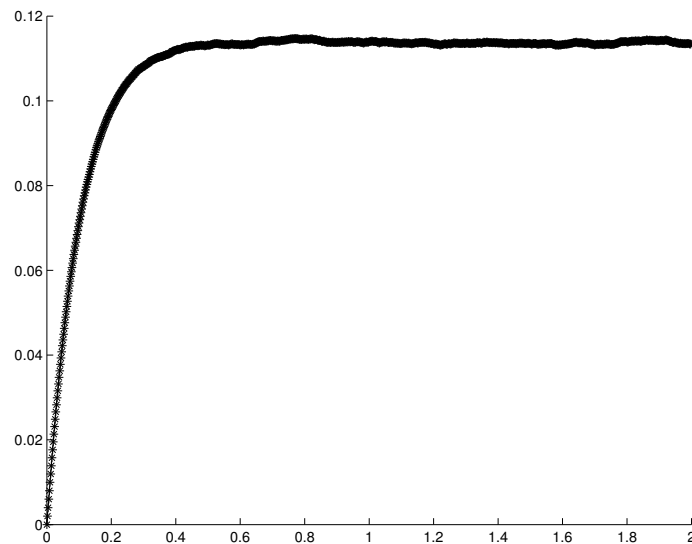


Figure 5: Time history of u at the middle point of the channel $y = \frac{1}{2}$. Solid line is the result for Hookean model using HMM. Dotted line is the result for Newtonian fluid. $De = 10^{-9}$, $Re = 1$, $\gamma = \frac{1}{9}$. This calculation relies essentially on the multiscale techniques discussed in the text.

Numerical Test 3: Augmented system (20) with HMM. The application of HMM allows us to simulate at significantly smaller De . The results are presented in Figures 5. These calculations are impossible without using HMM.

It is shown in the appendix that the Hookean model converges to the Newtonian fluid in the zero Deborah number limit, and so does FENE with a renormalized viscosity. The simplified momentum equation is

$$\frac{\partial u}{\partial t} + c = \frac{(1 - \gamma)C_{\bar{Q}} + \gamma \partial^2 u}{Re \partial y^2} \quad (21)$$

where $C_{\bar{Q}}$ is defined in appendix.

4 Numerical tests on a two-dimensional example

In this section we test the ideas discussed earlier on a full two dimensional example: the driven cavity flow. The equations now are (1), (2). The computational domain is taken to be the unit square $[0, 1] \times [0, 1]$. The boundary conditions are $\mathbf{u} = 0$ except at the top where $u = 1$. The parameters are chosen as $Re = 1$, $De = 10^{-11}$, $\gamma = \frac{1}{9}$. For the equation of \mathbf{u} , projection method on a staggered grid is used [12]. For the equation of \mathbf{Q} , first order upwind scheme is used for the convective term, and the Euler scheme is used to discretize the SDEs. The unit square $[0, 1] \times [0, 1]$ is divided into a 128×128 mesh. The macro time step-size is set as $\Delta t = 0.0001$, while the micro time step-size is set at $\delta t = 0.05 \times De$. $N_f = 200$ fields are used. At every macro time step, the micro-scale process for \mathbf{Q} is evolved for 20 micro time steps. The results of the last 5 steps are averaged to get the polymer stress.

We compare the results of Hookean dumbbell model, the Oldroyd-B model and the Newtonian fluid. In Figure 6 we plot the history of speed u and v at the points $(x, y) = (\frac{3}{4}, \frac{1}{4})$ and $(x, y) = (\frac{3}{4}, \frac{3}{4})$. We can see that the results of the Hookean dumbbell model agree well with that of the Newtonian fluid.

Figure 7 shows the streamline of Hookean dumbbell model at $t = 0.095$.

We also experimented with the FENE model. Our results are consistent with those presented earlier, and are therefore omitted from here.

5 Conclusion

In this paper, we explored BCF at small Deborah number. We used a stochastic multi-scale decomposition with an auxiliary fields in the equation for the configura-

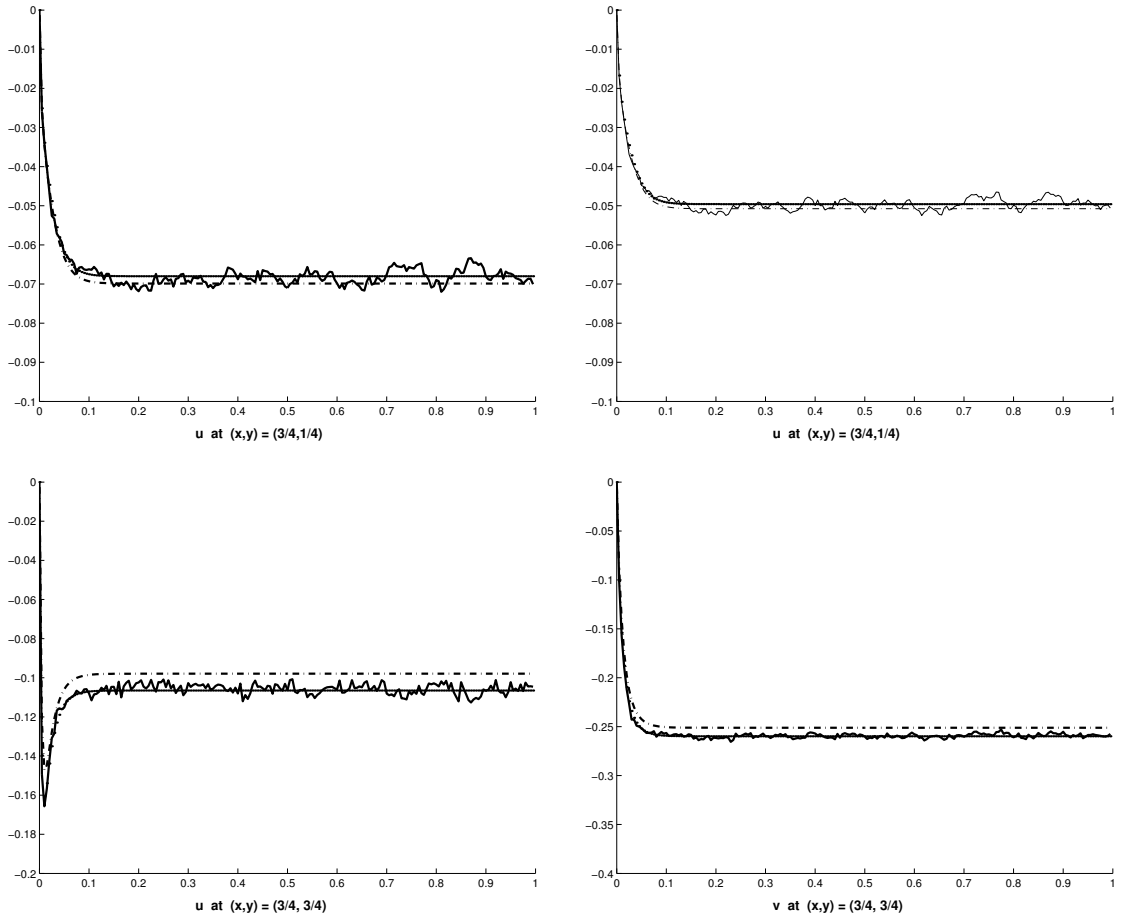


Figure 6: Time history of velocity u , v . Solid - Hookean, Dotted - Oldroyd-B, Dashed - Newtonian. Upper Left - u at $(\frac{3}{4}, \frac{1}{4})$; upper Right - v at $(\frac{3}{4}, \frac{1}{4})$; lower Left - u at $(\frac{3}{4}, \frac{3}{4})$; lower Right - v at $(\frac{3}{4}, \frac{3}{4})$.

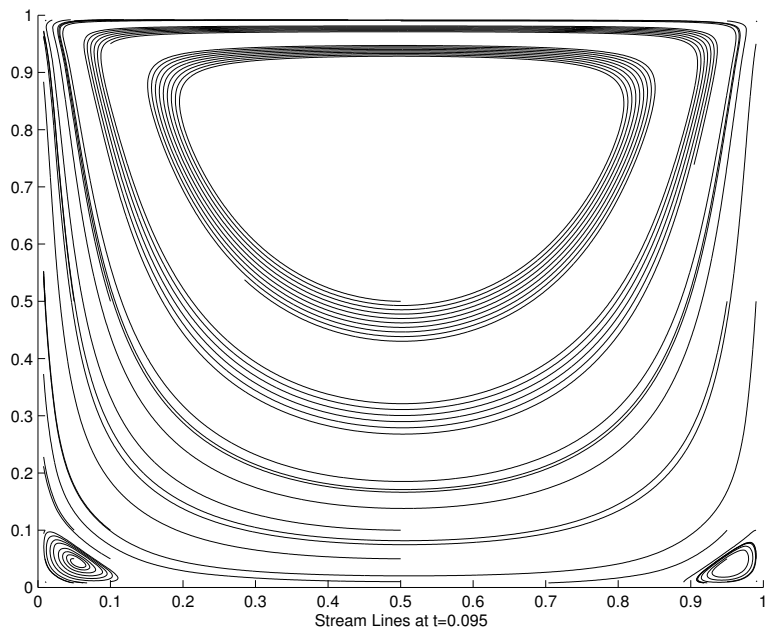


Figure 7: Streamlines of Hookean model at $t = 0.095$. $De = 10^{-11}$, $Re = 1$, $\gamma = \frac{1}{9}$.

tion fields and this technique greatly reduced the variance in the numerical results. HMM is applied to efficiently deal with the separation of time scales.

Acknowledgments

We thank Yannis Kevrekidis for pointing to us some of the references on BCF. E. V.-E. is partially supported by NSF grant DMS02-09959 and by AMIAS (Association of Members of the Institute for Advanced Study). W. E is partially supported by ONR grant N00014-01-1-0674 and National Science Foundation of China Class B Grant for Distinguished Young Scholars 10128102. P. Z. is partially supported by the special funds for Major State Research Projects G1999032804 and the Teaching and Research Award for outstanding young teachers from the Chinese MOE.

Appendix: The zero Deborah number limit

The zero Deborah number limit of BCF can be readily computed using (2) together with the enlarged system (13), (14) instead of (1). We start from the following

equation for $\mathbf{S} = \langle \bar{\mathbf{Q}} \otimes \mathbf{q} \rangle + \langle \mathbf{q} \otimes \bar{\mathbf{Q}} \rangle$ obtained from (13) and (14):

$$\begin{aligned} \frac{\partial}{\partial t} \mathbf{S} + (\mathbf{u} \cdot \nabla) \mathbf{S} &= \frac{1}{De} (\kappa \mathbf{C}_{\bar{\mathbf{Q}}} + \mathbf{C}_{\bar{\mathbf{Q}}} \kappa^T) + \kappa \langle \mathbf{q} \otimes \bar{\mathbf{Q}} \rangle + \langle \bar{\mathbf{Q}} \otimes \mathbf{q} \rangle \kappa^T \\ &\quad - \frac{1}{2De} (\langle \mathbf{q} \otimes \mathbf{F}(\bar{\mathbf{Q}}) \rangle + \langle \mathbf{F}(\bar{\mathbf{Q}}) \otimes \mathbf{q} \rangle + \langle \mathbf{G} \otimes \bar{\mathbf{Q}} \rangle + \langle \bar{\mathbf{Q}} \otimes \mathbf{G} \rangle), \end{aligned} \quad (22)$$

where $\mathbf{C}_q = \langle \mathbf{q} \otimes \mathbf{q} \rangle$, $\mathbf{C}_{\bar{\mathbf{Q}}} = \langle \bar{\mathbf{Q}} \otimes \bar{\mathbf{Q}} \rangle$. From (16) and the symmetry of τ_p , the sum of last four terms at the right hand-side is precisely the leading order term of τ_p/De^2 ; therefore, (5) implies that, to leading order in De ,

$$\frac{1}{De} \tau_p = \kappa \mathbf{C}_{\bar{\mathbf{Q}}} + \mathbf{C}_{\bar{\mathbf{Q}}} \kappa^T = C_{\bar{\mathbf{Q}}} (\kappa + \kappa^T), \quad (23)$$

where we used $\mathbf{C}_{\bar{\mathbf{Q}}} = C_{\bar{\mathbf{Q}}} \mathbf{I}$ which follows from the isotropy of the forcing, $\mathbf{F}(\mathbf{Q}) = \nabla_{\mathbf{Q}} V(\mathbf{Q})$. (23) implies that in the limit as $De \rightarrow 0$, (2) reduces to

$$\frac{\partial \mathbf{u}}{\partial t} + (\mathbf{u} \cdot \nabla) \mathbf{u} + \nabla p = \frac{\gamma}{Re} \Delta \mathbf{u} + \frac{(1-\gamma)C_{\bar{\mathbf{Q}}}}{Re} \Delta \mathbf{u}, \quad \nabla \cdot \mathbf{u} = 0. \quad (24)$$

This is the standard Navier-Stokes equation with a new (renormalized) viscosity. Furthermore, since the equilibrium density for (13) is (using $\mathbf{F}(\mathbf{Q}) = \nabla_{\mathbf{Q}} V(\mathbf{Q})$)

$$\rho(\bar{\mathbf{Q}}) = Z^{-1} e^{-V(\bar{\mathbf{Q}})}, \quad \text{with} \quad Z = \int e^{-V(\bar{\mathbf{Q}})} d^d \bar{\mathbf{Q}}, \quad (25)$$

For Hookean model, one obtains $Z = (\sqrt{2\pi})^d$, and

$$C_{\bar{\mathbf{Q}}} = \frac{1}{d} \langle \bar{\mathbf{Q}}^2 \rangle_{\rho} = 1 \quad (26)$$

which means that Hookean dumbbell model will converge to Newtonian flow in the zero Deborah number limit, while for FENE model, one can also obtain a close form of $C_{\bar{\mathbf{Q}}}$

$$C_{\bar{\mathbf{Q}}} = \frac{1}{d} \langle \bar{\mathbf{Q}}^2 \rangle_{\rho} = \frac{Q_0^2}{Q_0^2 + d + 2}. \quad (27)$$

It is easy to find that $C_{\bar{\mathbf{Q}}}$ is a monotonely increasing function of Q_0 , and $C_{\bar{\mathbf{Q}}} \sim 1$ as $Q_0 \rightarrow +\infty$.

References

- [1] R.B. Bird, O. Hassager, R.C. Armstrong and C.F. Curtiss, Dynamics of polymeric liquids; Vol. 2: kinetic theory (2nd ed.), Wiley-Interscience, New York, 1987.

- [2] J. Bonvin and M. Picasso, Variance reduction methods for CONNFFESSIT-like simulations, *J. Non-Newtonian Fluid Mech.*, 84(1999) 191-215.
- [3] M. Doi and S.F. Edwards, *The theory of polymer dynamics*, Oxford University Press, Oxford, 1986.
- [4] W. E, Analysis of the heterogeneous multiscale method for ordinary differential equations, submitted to *Comm. Math. Sci.* (2003).
- [5] W. E and B. Engquist, The heterogeneous multi-scale methods, to appear in *Comm. Math. Sci.* (2003).
- [6] P.G. de Gennes, *Scaling concepts in polymer physics*, Cornell Univ. Press, Ithaca, 1979.
- [7] M.A. Hulsen, A. P. G. van Heel and B. H. A. A. van den Brule, Simulation of viscoelastic flows using Brownian configuration fields, *J. Non-Newtonian Fluid Mech.*, 70(1997) 79-101.
- [8] M. Laso and H.C. Öttinger, Calculation of viscoelastic flow using molecular models: the CONNFFESSIT approach, *J. Non-Newtonian Fluid Mech.*, 47(1993) 1-20.
- [9] H.C. Öttinger, *Stochastic processes in polymeric liquids*, Springer-Verlag, Berlin and New York, 1996.
- [10] H.C. Öttinger, B.H.A.A. van den Brule, M.A.Hulsen, Brownian configuration fields and variance reduced CONNFFESSIT, *J. Non-Newtonian Fluid Mech.*, 70(1997) 255-261.
- [11] B. Oksendal, *Stochastic differential equations: an introduction with applications*(5th ed.), Springer-Verlag, Berlin and New York, 1998.
- [12] R. Peyret and T.D. Taylor, *Computational Methods for Fluid Flows*, Springer-Verlag, New York, 1983.
- [13] P.E. Kloeden and E. Platen, *Numerical solution of stochastic differential equations*, Springer-Verlag, Berlin and New York, 1995.
- [14] J.K.C. Suen, Y.L. Joo and R.C. Armstrong, Molecular orientation effects in viscoelasticity, *Annu. Rev. Fluid Mech.*, 34(2002) 417-444.

- [15] E. Vanden-Eijnden, Numerical techniques for multi-scale dynamical systems with stochastic effects, to appear in *Comm. Math. Sci.* (2003).